Materials Research. 2022; 25:e20220245
DOI: https://doi.org/10.1590/1980-5373-MR-2022-0245

TiO_2 Antireflection Coating Deposited by Electro-Beam Evaporation: Thin Film Thickness Effect on Weighted Reflectance and Surface Passivation of Silicon Solar Cells

José Cristiano Mengue Model[a], Adriano Moehlecke[a]*, Izete Zanesco[a], Moussa Ly[a], Tatiana Lisboa Marcondes[a]

[a]*Pontifícia Universidade Católica do Rio Grande do Sul, Escola Politécnica, Núcleo de Tecnologia em Energia Solar, Av. Ipiranga, 6681, P.96A, 90619-900, Porto Alegre, RS, Brasil.*

Received: May 18, 2022; Revised: September 21, 2022; Accepted: October 04, 2022

Titanium dioxide was extensively used in solar cell industry and currently has been studied to produce passivated contacts in PERC/PERT and TOPCon solar cells. The aim of this paper was to analyze the impact of the thickness of TiO_2 thin films deposited by electro-beam evaporation on the weighted reflectance and the surface passivation on silicon solar cells. Thin films with different thicknesses were deposited to produce PERT solar cells, varying from 50 to 90 nm. The surface passivation was enhanced as the thickness was increased. For instance, at 400 nm, the internal quantum efficiency increased from 71% to 76% when the thickness of the TiO_2 was augmented from 50 nm to 90 nm. The lowest weighted reflectance was obtained in samples with 80 nm thick TiO_2 films. Considering the compromise between antireflection properties and surface passivation, the highest efficiency solar cells were produced with 80 nm thick TiO_2.

Keywords: *Silicon solar cells, titanium dioxide, antireflection coating, surface passivation.*

1. Introduction

In the last decades, most of solar cell industries used the n^+pp^+ standard structure and front surface passivation based on silicon nitride (SiNx) deposited by plasma enhanced chemical vapor deposition (PECVD). The rear face was covered by a screen-printed Al thick film and with a thermal process, the back surface field (BSF) was formed[1,2]. To reach higher efficiencies, advanced structures like PERC (passivated emitter and rear cell) and PERT (passivated emitter rear totally diffused)[3,4] or TOPCon (tunnel oxide passivated contacts)[5] have been introduced in the production lines. For instance, the market share of PERC solar cells grew from 21% in 2017 to 80% in 2020[6]. High volume production allows the implementation of more complex solar cell structures and the use of high-quality materials, maintaining the low-cost production.

The silicon surface passivation is an important step in the production of PERC/PERT and TOPCon solar cells. As the surfaces in a solar cell form a discontinuity to the semiconductor lattice, several dangling bonds are produced[7]. Therefore, minority charge carriers can recombine in the silicon wafer surface. The silicon nitride was the preferred material used in the last decades to reduce the surface recombination of the n^+ doped surface, that forms the front face on the n^+pp^+ phosphorus/aluminum solar cells[7]. Three main reasons for the use of SiNx can be mentioned: 1) the refractive index allows the production of excellent antireflection coating (ARC) for silicon solar cells; 2) the PECVD technique produces hydrogen during the deposition, which can passivate surface defects; 3) the positive charges presented in the SiN_x films deposited by PECVD reduce the hole concentration (minority carrier) near the surface and therefore diminish the surface recombination.

The PERC solar cells need effective surface passivation in both faces of the solar cell and other materials then SiNx have been studied. The Al_2O_3 layers deposited by PECVD or by atomic layer deposition (ALD) have been implemented to passivate p-type furnaces bearing in mind that negative charges are produced, keeping away the minority charge carriers (electrons) from the surface[7]. The thermally grown SiO_2 also has been proposed to passivate n-type and p-type surfaces[8,9]. The SiO_2 was the main passivating layer used in laboratories to obtain high efficiency devices. For PERC solar cells, front and rear surfaces can be passivated in only one thermal step after dopant diffusion. Besides, non-stoichiometric SiOx films can also be used to passivate contacts in TOPCon solar cells[5,8].

The TiO_2 was extensively used by the PV industry until mid-1990's as an ARC. These thin films present high refractive index that is optimal for reducing reflection losses of glass-encapsulated solar cells, low extinction factor, high thermal stability, and high resistance to chemical[10-12]. Many deposition techniques have been used to obtain TiO_2 films. The atmospheric pressure vapor deposition (APCVD) was the technique employed in most industries to obtain ARC TiO_2 films due to high throughput and low cost. The ALD is the technique more studied because higher surface passivation is obtained, but with the demerits of time consuming and the complex post process to reduce the surface recombination[13]. The pulsed laser deposition (PLD) method has been also studied to obtain TiO_2 compound thin films to produce ARC

*e-mail: moehleck@pucrs.br

in solar cells or TCOs (transparent conductor oxides)[14-16]. The high vacuum evaporation was used to deposit ARC TiO_2 films, but surface passivation was not analyzed[12,13,17,18].

The aim of this paper is to analyze the influence of the TiO_2 thickness, when deposited by electron-beam evaporation on the weighted reflectance and the surface passivation of n^+ doped surfaces as well as on the electrical parameters of PERT silicon solar cells.

2. Materials and Methods

2.1. Solar cell fabrication process

Solar grade silicon wafers, with 100 mm diameter, grown by the Czochralski technique, p-type, boron doped, were used. The steps of the solar cell fabrication process are presented in Figure 1[19-21].

The silicon wafers were textured in a solution of KOH, isopropyl alcohol and deionized water and cleaned in the RCA solution[22].

A liquid containing boron (PBF20, Filmtronics) was spun-on on one side of the wafers and they were introduced in an oven for evaporation of solvents. Boron was diffused into the silicon wafers in a quartz tube furnace at 970 °C[19,20]. To produce the n^+ emitter, phosphorus was diffused at 845 °C in a quartz tube by using $POCl_3$ as source. After each diffusion step (boron and phosphorus), the phosphorus and boron silicates were etched by immersion of the wafers in HF solution followed by RCA chemical cleaning.

The TiO_2 films were deposited on the front face of the silicon wafers by electron-beam evaporation in a Temescal BJD2000 system. The 99.9% pure TiO_2 pellets were placed in a graphite crucible and the material was melted in a chamber maintained under pressure of around 8.5×10^{-5} torr. The deposition rate of the material was maintained at 1 Å / s. The thickness of TiO_2 films ranged from 50 nm to 90 nm. Four devices for each thickness were fabricated.

Metal grid was deposited by screen-printing: Ag on the front and Al/Ag paste on the rear face. The pastes were dried in a belt furnace and were fired at 860 °C[20]. To finish the manufacturing process, the solar cells were cut in a pseudo-square format by laser, obtaining devices with an area of 61.58 cm^2. The Figure 2 illustrates the solar cell structure with TiO_2 thin film.

2.2. Characterization of solar cells and TiO_2 coatings

All devices were characterized under standard conditions (100 mW/cm^2, AM1.5G and 25 °C) in a solar simulator calibrated with silicon solar cells previously measured at CalLab - FhG-ISE (*Fraunhofer-Institut für Solare Energiesysteme*), Germany. The short-circuit current density (J_{SC}), the open circuit voltage (V_{OC}), fill factor (FF) and the efficiency (η) were determined from the I-V curve. The spectral response (SR) and hemispherical reflectance (ρ) were measured in a PVE300 photovoltaic QE system (Bentham Instruments), to obtain the internal quantum efficiency. Considering SR, reflectance and solar spectrum AM 1.5G, the weighted reflectance (ρ_w) was calculated, according to the following equation[23]:

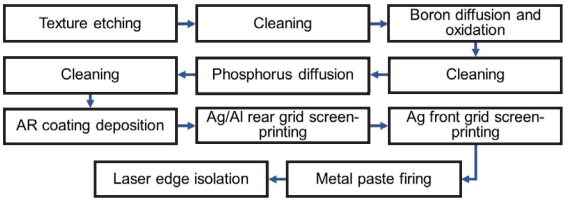

Figure 1. Fabrication process sequence of the TiO_2 coated PERT solar cells.

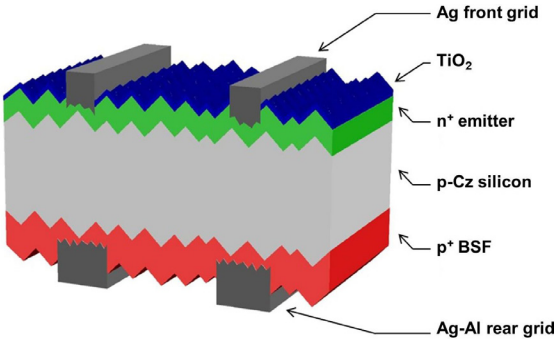

Figure 2. Structure of TiO_2 coated PERT solar cells.

$$\rho_W = \frac{\int_{\lambda_1}^{\lambda_2} G(\lambda)\rho(\lambda)SR(\lambda)d\lambda}{\int_{\lambda_1}^{\lambda_2} G(\lambda)SR(\lambda)d\lambda} \quad (1)$$

Where G(λ) is the AM1.5G spectral irradiance, SR(λ) is the spectral response of the solar cell and ρ(λ) is the reflectance.

The TiO_2 thin films were also deposited on n-type silicon textured wafers and the hemispherical reflectance was measured in five points of the wafers, after the deposition and after the firing process. The firing process was carried out after the metal grid screen-printing and the high temperature of the process may modify the film characteristics.

The SEM images of textured silicon wafers were obtained as well as TEM images of textured samples coated with 80 nm TiO_2 thick film. SEM images were obtained with a Inspect-S50 FEG and TEM ones with TECNAI, 200kV.

3. Results and Discussion

Figure 3 is an SEM image showing the sample cross-section after KOH etching, where the morphological change from a plane substrate to a pyramidal structure can be observed. The structures in the homogeneous textured morphology have a dimension of 5-8 µm. The Figures 4, a-c, present the hemispherical reflectance of the textured silicon wafers with TiO_2 thin films of different thicknesses. Higher thickness implies in minimum reflectances for longer wavelengths. The firing process at 860 °C produces a wavelength (λ_{min}) shift of the minimum spectral reflectance of around 40 nm. The physical mechanisms to explain this change is the reduction of the film thickness and/or the increase of refractive index[24-28]. The thermal process (sintering) in temperatures above 700 °C results in significant densitification of the TiO_2 layer and there

is a linear relationship between density and refractive index of a TiO_2 thin film[26]. For instance, for TiO_2 films deposited by APCVD (atmospheric pressure chemical vapour deposition), the authors commented that heat treatments reduced the thickness and increased the refractive index, explained by a phase transition from amorphous to partially crystalline[25]. The Figure 4-c shows the reflectance of 80 nm thick TiO_2 films and the shift in the wavelength of the minimum reflectance. The Table 1 summarizes the wavelength of the minimum spectral reflectance and the weighted reflectance for each ARC. The value of the lower ρ_w, before and after firing process, was found in the thin film with as-deposited thickness of 80 nm, achieving ρ_w of around 1.3%.

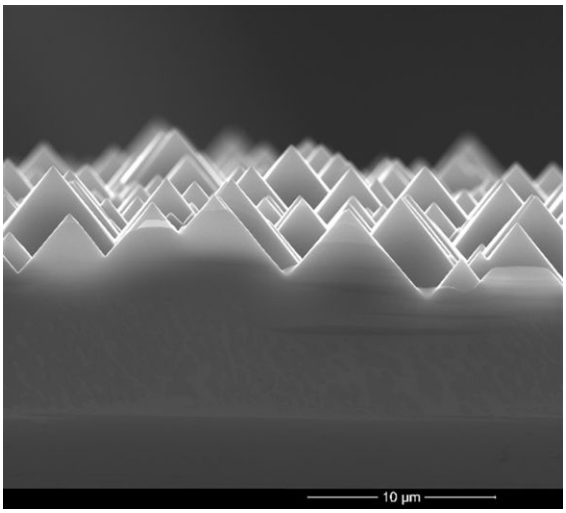

Figure 3. Cross-sectional MEV image of the textured silicon wafer. The pyramid heights vary from 5-8 µm.

Table 1. The wavelength of the minimum spectral reflectance and weighted reflectance for textured silicon wafers coated with TiO_2 films deposited by e-beam evaporation. d_{TiO2} is the thin film thickness measured after the e-beam evaporation.

d_{TiO2} (nm)	Before firing		After firing	
	λ_{min} (nm)	ρ_w (%)	λ_{min} (nm)	ρ_w (%)
50	530 ± 11	2.2 ± 0.1	490 ± 10	3.1 ± 0.2
60	635 ± 15	1.7 ± 0.1	580 ± 13	2.0 ± 0.1
65	680 ± 23	1.8 ± 0.2	635± 18	1.9 ± 0.1
70	700 ± 18	2.0 ± 0.2	660 ± 18	1.9 ± 0.1
80	690 ± 12	1.2 ± 0.1	670 ± 14	1.3 ± 0.1
90	740 ± 11	1.2 ± 0.2	710 ± 30	1.9 ± 0.4

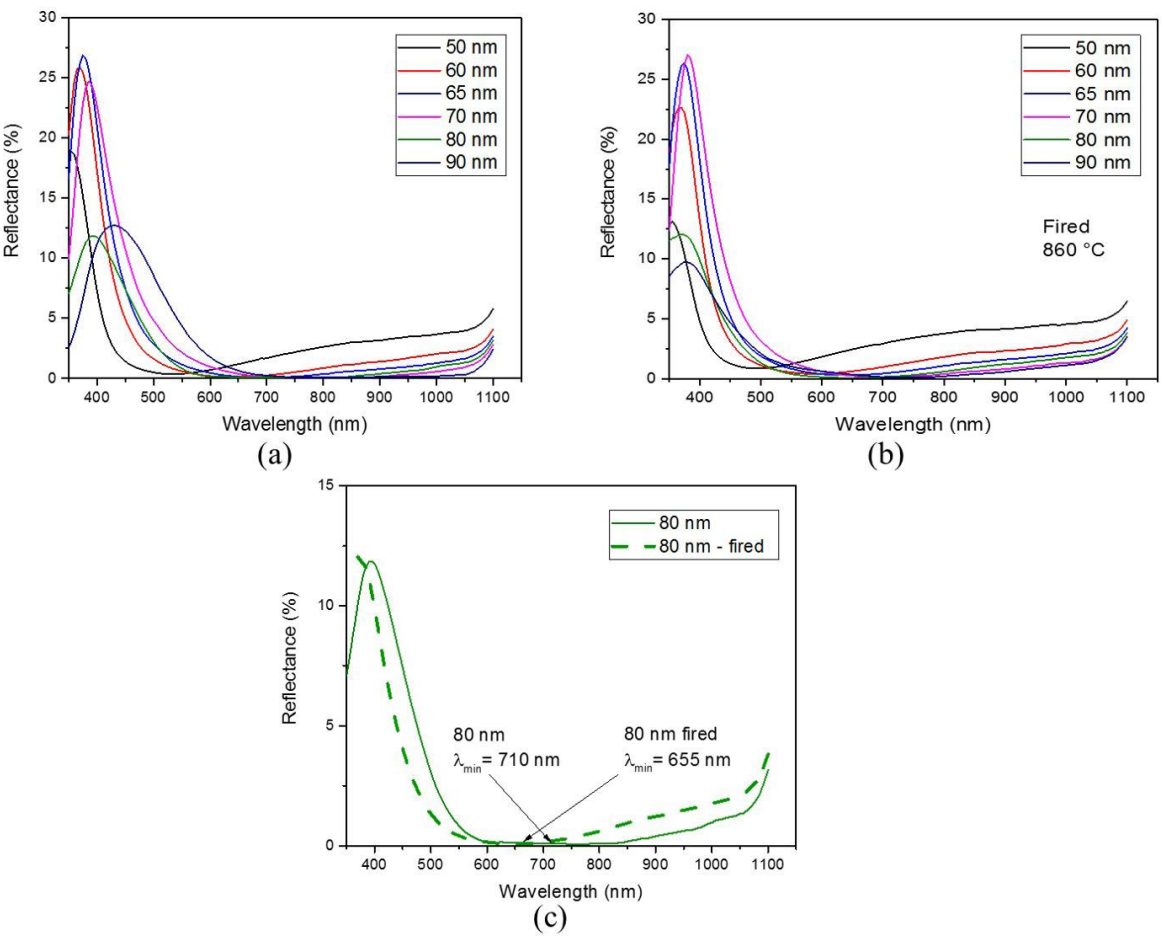

Figure 4. Reflectance of TiO_2 coated textured silicon wafers (a) before, (b) after a thermal process at 860 °C (metal paste firing) and (c) for 80 nm thick films (before and after firing).

Figures 5 are TEM cross-sectional images showing the interface between the silicon substrate and the TiO_2 film sintered at 860 °C. The film thickness is 80 nm as shown in Figure 5-a. The interface between the silicon substrate and the film is homogeneous, indicating a good adhesion between the film and the substrate, as it can be observed in Figure 5-b. The film contrast in the images indicates the presence of voids, even though the thermal process promoted a film densification.

The Figure 6 presents the electrical parameters of solar cells coated with the TiO_2 of different thickness. The average values of four solar cells as well as the electrical parameters

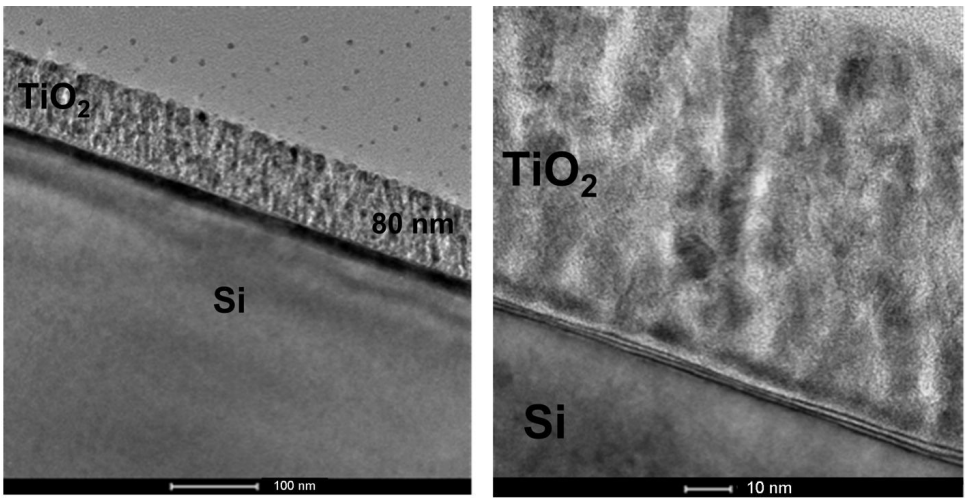

Figure 5. TEM cross-sectional image of a textured silicon wafer covered with 80 nm thick TiO_2 film, after deposition process at 860 °C. The scale bar is equivalent to 100 nm (a) and 10 nm (b).

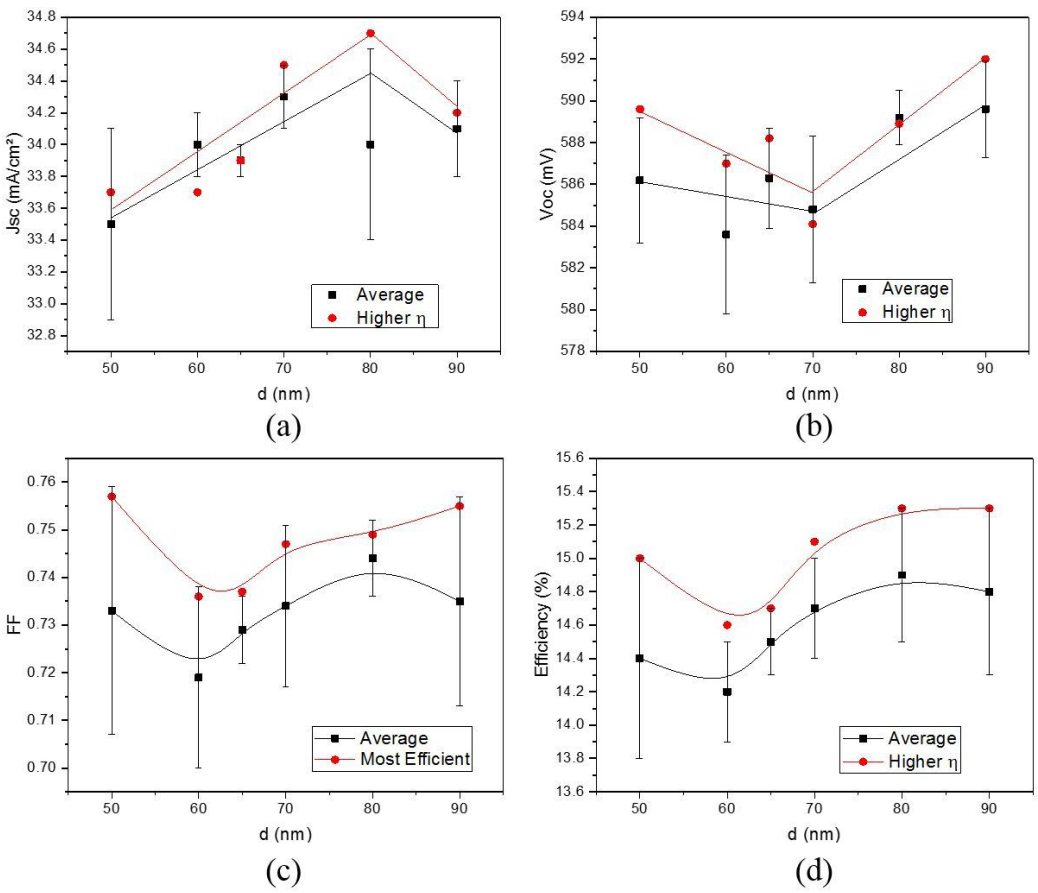

Figure 6. (a) J_{SC}, (b) V_{OC}, (c) FF and (d) efficiency of solar cells produced as a function of TiO_2 film thickness.

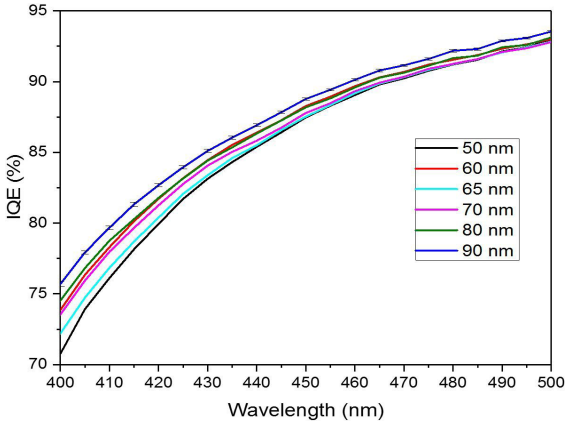

Figure 7. IQE in the range of 400 nm to 500 nm for solar cells with different thickness of TiO_2 layer. Error bar over the line corresponding to 90 nm thick films are shown.

of the highest efficiency devices are presented. The most efficient solar cell with 80 nm thick layer presented the J_{SC} 1.0 mA/cm^2 higher than those with 50 nm layer, agreeing with the lowest weighted reflectance observed. Concerning the V_{OC}, the highest values were observed for devices with TiO_2 90 nm thick layers, which can indicate a better surface passivation. As a result, the efficiency of the devices increased from 15.0% (50 nm TiO_2 layer) to 15.3% (80 nm and 90 nm thick layers). Then, the high thicknesses of TiO_2 lead to similar values of the efficiency due to the improvement of the J_{SC} and the V_{OC}. The enhancement in the efficiency of 0.3% (absolute) represents an increasing of 0.13 W in each solar cell of 210 mm x 210 mm (dimensions of M12 industrial solar cell) and an increasing of around 9.4 W in a standard photovoltaic module with 72 cells (power of around 476 W), at standard conditions. Therefore, 0.3% could be relevant in a large-scale production of photovoltaic modules.

In the Figure 7 is presented the internal quantum efficiency (IQE) of solar cells with higher efficiencies produced with TiO_2 films deposited by e-beam. The IQE for shorter wavelengths is increased as the thickness of the TiO_2 is augmented. For instance, at 400 nm, the IQE enhances from 71% to 76% when the thickness of the TiO_2 was increased from 50 nm to 90 nm. The error due to the IQE measurements is of around 0.5% at 400 nm. Therefore, the thick TiO_2 films provided better surface passivation. To compare the surface passivation, similar solar cells with a thermally grown SiO_2 and TiO_2 ARC achieved an IQE of around 80% at 400 nm, with one extra thermal step to obtain the SiO_2 layer[29].

4. Conclusions

The TiO_2 films deposited by e-beam vacuum evaporation were analyzed considering weighted reflectance, surface passivation and electrical parameters of n^+pp^+ silicon solar cells. Thickness of the films was ranged from 50 nm to 90 nm and the higher internal quantum efficiency for shorter wavelengths shows that surface passivation was enhanced for thicker films. For instance, 40 nm thicker films imply an increase of 4% (absolute) in the internal quantum efficiency for a wavelength of 400 nm. The thickness of 80 nm produced the lowest weighted reflectance and the highest efficiency solar cells.

5. Acknowledgments

The authors acknowledge the financial support provided by the Brazilian financing agencies CNPq and CAPES and by the Brazilian utility Eletrosul Centrais Elétricas S. A.

6. References

1. Battaglia C, Cuevas A, Wolf S. High-efficiency crystalline silicon solar cells: status and perspectives. Energy Environ Sci. 2016;9:1552-76.
2. Moehlecke A, Zanesco I. Development of silicon solar cells and photovoltaic modules in Brazil: analysis of a pilot production. Mater Res. 2012;15(4):581-8.
3. Zhang Y, Wang L, Chen D, Kim M, Hallam B. Pathway towards 24% efficiency for fully screen-printed passivated emitter and rear contact solar cells. J Phys D Appl Phys. 2021;54(21):214003.
4. Balaji N, Lai D, Shanmugam V, Basu PK, Khanna A, Duttagupta S, et al. Pathways for efficiency improvements of industrial PERC silicon solar cells. Sol Energy. 2021;214:101-9.
5. Kafle B, Goraya BS, Mack S, Feldmann F, Nold S. TOPCon – Technology options for cost efficient industrial manufacturing. Sol Energy Mater Sol Cells. 2021;227:111100.
6. ITRPV: International Technology Roadmap for Photovoltaic [homepage on the Internet]. 2021 [cited 2022 May 18]. Available from: http://itrpv.vdma.org.
7. Bonilla RS, Hoex B, Hamer P, Wilshaw PR. Dielectric surface passivation for silicon solar cells: a review. Phys Status Solidi, A Appl Mater Sci. 2017;214(7):1700293.
8. Glunz SW, Feldmann F. SiO_2 surface passivation layers – a key technology for silicon solar cells. Sol Energy Mater Sol Cells. 2018;185:260-9.
9. Zhuang YF, Zhong SH, Liang XJ, Kang HJ, Li ZP, Shen WZ. Application of SiO_2 passivation technique in mass production of silicon solar cells. Sol Energy Mater Sol Cells. 2019;193:379-86.
10. Richards BS. Comparison of TiO_2 and other dielectric coatings for buried-contact solar cells: a review. Prog Photovolt Res Appl. 2004;12:253-81.
11. Cui J, Allen T, Wan Y, Mckeon J, Samundsett C, Yan D, et al. Titanium oxide: a re-emerging optical and passivating material for silicon solar cells. Sol Energy Mater Sol Cells. 2016;158:115-9.
12. Zanesco I, Moehlecke A, Model JCM, Ly M, Aquino J, Razera RAZ, et al. Evaluation of the TiO2 anti-reflective coating in PERT Solar cells with silicon dioxide passivation. In: Solar World Congress; Santiago. Proceedings. Freiburg: ISES; 2019.
13. Liao B, Hoex B, Aberle AG, Chi D, Bhatia CS. Excellent c-Si surface passivation by low-temperature atomic layer deposited titanium oxide. Appl Phys Lett. 2014;104:253903. http://dx.doi.org/10.1063/1.4885096
14. Haider AJ, Najim AA, Muhi MAH. TiO_2/Ni composite as antireflection coating for solar cell application. Opt Commun. 2016;370:263-6. http://dx.doi.org/10.1016/j.mssp.2017.08.035
15. Najim AA. Synthesis and characterizations of $(\delta\text{-}Bi_2O_3)_{0.93}(TiO_2)_{0.07}$ thin films grown by PLD technique for optoelectronics. Mater Sci Semicond Process. 2017;71:378-81. http://dx.doi.org/10.1016/j.optcom.2016.03.034
16. Gbashi KR, Najim AA, Muhi MAH, Salih AT. Structural, morphological, and optical properties of nanocrystalline $(Bi_2O_3)_{1-x}$:$(TiO_2)_x$ thin films for transparent electronics. Plasmonics. 2019;14:623-30. http://dx.doi.org/10.1007/s11468-018-0840-1
17. Rao KN, Mohan S. Optical properties of electron-beam evaporated TiO_2 films deposited in an ionized oxygen medium. J Vac Sci Technol. 1990;A8:3260-4.

18. Cahill DG, Allen TH. Thermal conductivity of sputtered and evaporated SiO_2 and TiO_2 optical coatings. Appl Phys Lett. 1994;65:309-11.
19. Zanesco I, Moehlecke A. Impurity diffusion process in silicon wafers to fabricate solar cells (Processo de difusão de dopantes em lâminas de silício para a fabricação de células solares). Brazilian patent PI12030606, BR 10 2012 030606 9. 2012, Nov 30.
20. Zanesco I, Moehlecke A. Analysis of the silicon dioxide passivation and forming gas annealing in silicon solar cells. In: Solar World Congress; 2015 Nov 8-12; Daegu, Korea. Proceedings. Freiburg: SES; 2015 [cited 2022 May 18]. Available in: http://proceedings.ises.org/paper/swc2015/swc2015-0035-Zanesco.pdf
21. Crestani T, Zanesco I, Moehlecke AL. Analysis of the boron concentration profile to produce p-type silicon solar cells by reducing thermal steps. In: XLI Reunión de Trabajo de la Asociación Argentina de Energías Renovables y Medio Ambiente. Proceedings. Cordoba: ASADES; 2018.
22. Kern W. Handbook of semiconductor wafer cleaning technology. New Jersey: Noyes Publications; 1998.
23. Zhao J, Green MA. Optimized antireflection coatings for high-efficiency silicon solar cells. IEEE Trans Electron Dev. 1991;38(8):1925-34.
24. Ly M, Eberhardt D, Filomena GZ, Moehlecke A, Zanesco I. Impact of metal grid firing on antireflection coatings. In: 22th European Photovoltaic Solar Energy Conference and Exhibition; Milan. Proceedings. Milan: WIP; 2007. p. 1532-4.
25. Vallejo B, Gonzalez-Mañas M, Martínez-López J, Morales F, Caballero MA. Characterization of TiO_2 deposited on textured silicon wafers by atmospheric pressure chemical vapour deposition. Sol Energy Mater Sol Cells. 2005;86:299.
26. Richards BS. Single-material TiO_2 double-layer antireflection coatings. Sol Energy Mater Sol Cells. 2003;79:369-90.
27. Sério S, Jorge MEM, Maneira MJP, Nunes Y. Influence of O_2 partial pressure on the growth of nanostructured anatase phase TiO_2 thin films prepared by DC reactive magnetron sputtering. Mater Chem Phys. 2011;126:73-81.
28. Zambrano DF, Villarroel R, González RE, Carvajal N, Rosenkranz A, Montaño-Figueroa AG, et al. Mechanical and microstructural properties of broadband anti-reflective TiO_2/SiO_2 coatings for photovoltaic applications fabricated by magnetron sputtering. Sol Energy Mater Sol Cells. 2021;220:110841.
29. Moehlecke A, Marcondes TL, Aquino J, Zanesco I, Ly M. Cost-effective thin n-type silicon solar cells with rear emitter. Mater Res. 2020;23(1):e20190536.